Effect of power on the growth of nanocrystalline silicon films

2008 J. Phys.: Condens. Matter 20 335215

(http://iopscience.iop.org/0953-8984/20/33/335215)

J. Phys.: Condens. Matter **20** (2008) 335215 (7pp) doi:10.1088/0953-8984/20/33/335215

Effect of power on the growth of nanocrystalline silicon films

Sushil Kumar[1], **P N Dixit, C M S Rauthan, A Parashar and Jhuma Gope**

Plasma Processed Materials Group, National Physical Laboratory, Dr K S Krishnan Road, New Delhi 110 012, India

E-mail: skumar@mail.nplindia.ernet.in

Received 16 January 2008, in final form 7 June 2008
Published 28 July 2008
Online at stacks.iop.org/JPhysCM/20/335215

Abstract

Nanocrystalline silicon thin films were grown using a gaseous mixture of silane, hydrogen and argon in a plasma-enhanced chemical vapor deposition system. These films were deposited away from the conventional low power regime normally used for the deposition of device quality hydrogenated amorphous silicon films. It was observed that, with the increase of applied power, there is a change in nanocrystalline phases which were embedded in the amorphous matrix of silicon. Atomic force microscopy micrographs show that these films contain nanocrystallite of 20–100 nm size. Laser Raman and photoluminescence peaks have been observed at 514 cm^{-1} and 2.18 eV, respectively, and particle sizes were estimated using the same as 8.24 nm and 3.26 nm, respectively. It has also been observed that nanocrystallites in these films enhanced the optical bandgap and electrical conductivity.

1. Introduction

Hydrogenated amorphous silicon (a-Si:H) thin films grown by the plasma-enhanced chemical vapor deposition (PECVD) technique have opened a new window for the material scientists and engineers to understand the basics and to make various semiconducting devices using this material about thirty years ago. At the same time silicon nanostructures had also been observed by Veprek *et al* [1]. However, the potentiality of nanocrystalline silicon has not been realized since those days. Now nanocrystalline silicon seems to be overtaking amorphous silicon due to its stability and tailoring of the bandgap.

In recent years interest in the growth of nanocrystalline silicon (nc-Si:H) films has been generated for applications in electronic and optoelectronic devices [2–7]. This material is a promising candidate for such devices because of its wider bandgap and near-direct bandgap nature. It has also been shown that nc-Si:H films and related devices are more stable during light soaking than a-Si:H [5]. Orpella *et al* [6] have studied the stability of nc-Si:H thin film transistors (TFTs). Their studies show that TFTs made of nc-Si:H show more stability than a-Si:H TFTs under prolonged times of gate bias stress. However, the main difficulty with nc-Si:H (and perhaps also with other nanomaterials) is the precise control over nanosized grains and their uniform distribution, otherwise it is very difficult to get the desired properties.

We have grown nc-Si:H films on glass substrates over a large area (100 cm^2) in a PECVD system using deposition parameters away from the conventional low power regime normally used for the deposition of device quality a-Si:H films [8]. The effect of power on the properties of these nc-Si:H films will be presented in this paper. High pressure growth of nc-Si:H films has been presented elsewhere by us [9].

2. Experimental details

The PECVD system used for deposition of nc-Si:H films is a parallel plate capacitatively coupled. A detailed description of the system has been described elsewhere [10]. Substrates were placed on the ground electrode and radio-frequency rf power (13.56 MHz) was applied to the cathode electrode from 20 to 100 W over a 120 cm^2 electrode area. A gaseous mixture of silane, SiH_4 (5%, diluted in hydrogen H_2) and argon (Ar), was used as precursor for the deposition of nc-Si:H films at a fixed pressure of 0.7 Torr. Initially SiH_4 was introduced into the process chamber at a flow rate of 40 sccm and the corresponding pressure was noted as 0.133 Torr. Then the Ar was flowed into the process chamber and the pressure was

[1] Author to whom any correspondence should be addressed.

Table 1. Typical process parameters used for the deposition of nc-Si:H films.

Process parameters	Values
Base vacuum	7.5×10^{-7} Torr
Area of the electrode	120 cm^2
Gap between electrodes	1.2 cm
Substrate temperature	220 °C
Applied power	20–100 W
Flow rate (SiH_4)	40 sccm
Relative Ar partial pressure	0.25 Torr
Deposition pressure	0.7 Torr

adjusted with the help of a needle valve to 0.25 Torr. We call this pressure (0.25 Torr) the relative argon partial pressure. The deposition pressure of 0.7 Torr was achieved by adjusting the throttle valve with its controller and Baratron (all M/s MKS make). The typical process parameters used for discharge and other experimental details are shown in table 1.

The structural, optical and electrical properties of these films were investigated using atomic force microscopy (AFM), laser Raman spectroscopy, photoluminescence (PL), optical bandgap (E_g) and conductivity (σ) as a function of applied rf (13.56 MHz) power at a fixed relative Ar partial pressure of 0.25 Torr. Thicknesses of these films were in the range of 0.5–0.8 μm, measured using a Talystep, M/s Rank Tailor Hobson, UK. For morphological studies of these nc-Si:H films, an AFM (Molecular Imaging, USA) was used to record the images. The PL studies were conducted on a Perkin-Elmer LS-55 luminescence spectrometer. Raman scattering measurement was performed in the range 200–850 cm^{-1} using a Spex micro Raman set-up. The spectral dependence of optical reflection and transmission was recorded on a spectrophotometer (M/s Shimadzu, Japan, Model No. 3101 PC) for the estimation of E_g. The absorption coefficient (α) was estimated using the relation $T = (1 - R)^2 \exp(-\alpha d)$, where T is the transmission, R is the reflectance and d is the thickness of the film. The values of the bandgap (E_g) was evaluated from the intercept of Tauc's plot of $(\alpha h\nu)^{1/2}$ versus $h\nu$ (photon energy). Conductivity measurements were carried out using a Keithley 617 Programmable Electrometer on planar samples which were made by evaporating aluminum electrodes on nc-Si:H films in a vacuum of better than 10^{-5} Torr, having a gap of 0.078 cm and width of 1.0 cm.

3. Results and discussion

The deposition rate of the films was calculated from the measured total thickness and deposition time. Thicknesses of these films were estimated by step height measurement using Talystep (M/s Rank Tailor Hobson, UK) equipment. Variation of deposition rate of nc-Si:H films as a function of applied rf power is shown in figure 1. The deposition rate of these films increases from 1.5 to 5 Å s^{-1} as the applied rf power increases from 20 to 100 W. Increase of applied rf power enhances the dissociation and ionization of silane radicals and thus a resulting increase of the flux of depositing precursors to the substrate surface. Thus, the increased deposition rate with rf power is probably due to the increased

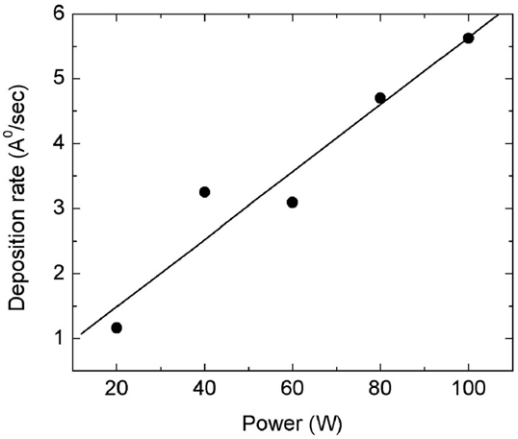

Figure 1. Variation of deposition rate of nc-Si:H films with applied power.

plasma density and also the Ar, allowing more efficient SiH_4 dissociation [11]. There are several deposition techniques including rf magnetron, hot wire CVD [12] and PECVD [13] that have been used to deposit nc-Si:H films at a deposition rate below 10 Å s^{-1} [14]. However, with the proper optimization of PECVD parameters one can obtain a deposition rate of the order of 10–30 Å s^{-1} [14]. Normally for the deposition of device quality amorphous silicon films low power density is applied to the cathode [8]. One can increase the deposition rate with the increase of applied power. However, use of a high power density is not recommended for achieving high deposition rates due to ionic bombardment of the growing film surface which may increase stresses and defects in the films [15]. Therefore, the high power regime in the PECVD system is not explored very well for the growth of silicon thin films. However, when we intentionally went on to apply high power to the cathode in our PECVD system, we have observed that high power is pertaining to the growth of nanosilicon films. Roca i Cabarrocas [16] has studied the effect of pressure on the deposition rate of films in a rf PECVD system at a fixed power density of 80 mW cm^{-2} and shown a change in the material from microcrystalline silicon at low pressure (less than 0.75 Torr) to polymorphous silicon at intermediate pressure (between 0.75 and 1.6 Torr) and then to amorphous silicon at high pressure (higher than 1.6 Torr) where powder formation takes place. Using the region of high pressure where powder formation takes place has been used as precursors and using a square wave modulated discharge one should be able to deposit silicon nanocrystals [17]. It is important to mention that direct gas-phase nucleation of nanocrystalline phases and later its incorporation in the film is undesirable from the point of view of controllability and reproducibility of the process. However, we are not very sure in our case about the nanoparticle formation in the gas phase or grown directly in the growing film surface on the substrate. This could be judged by laser scattering measurement of the silane plasma [18] which we have not carried out during the present investigation. There could be two mechanisms of powder formation in a silane plasma involving (i) charged particles [19] and (ii) neutral particles [20] by plasma polymerization. Primarily, clusters

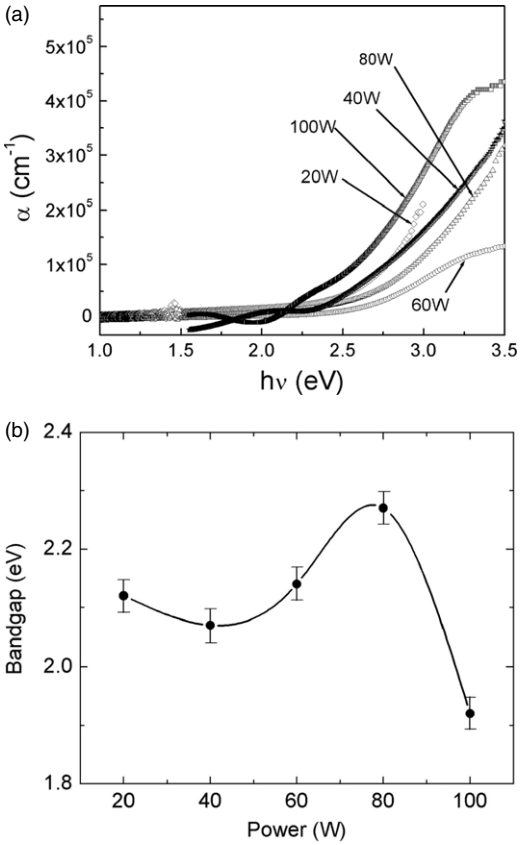

Figure 2. (a) Optical absorption coefficient as a function of photon energy of nc-Si:H films deposited at various powers. (b) Variation of optical bandgap of nc-Si:H films with applied power.

are formed as a result of molecular and ion polymerization chemistry. These clusters nucleate and grow into nanometer-sized structures with a diameter of 20–50 nm under some appropriate conditions. Then these nanometric-sized particles having positive or negative charges agglomerate at a critical density [19]. In the second mechanism neutral particles favor powder formation only by plasma polymerization, starting from SiH_x radicals [20]. We have used Ar dilution to avoid the aggregation of nanoparticles inside the plasma at high power condition. Since Ar dilution increases the average electron temperature by transforming its excitation energy it thereby causes dissociation of the precursor gas into reactive species. Ar ions with appropriate energy, in the case of nc-Si:H, favors reconstruction of strong Si–Si bonds by breaking weakly bonded Si–Si atoms. The role of Ar has also been seen in the growth of hard materials when it preferably etches weak bonds. In our case SiH_4 (5%) is also highly diluted in hydrogen which also favors the formation of crystallinity. Argon dilution of SiH_4 has also been suggested as an alternative to H_2 dilution for stable and high efficiency silicon thin film solar cells [21].

The plot of optical absorption coefficient (α) versus photon energy ($h\nu$) of nanocrystalline silicon thin films deposited at different rf powers is shown in figure 2(a). All these films exhibit high absorption (in the photon energy range from 2.25 to 3 eV) of the order of 10^5 cm^{-1}. In order to estimate the bandgap of the nanocrystalline silicon films $(\alpha h\nu)^{1/2}$ versus $h\nu$ (Tauc's model) has been plotted and extrapolated in the linear region. The trend of variation of bandgap with rf power can be seen in figure 2(b). The E_g values of these nc-Si:H films were found higher than those of a-Si:H films (normally in the range of 1.75 to 1.8 eV observed for films deposited in the low power regime in our PECVD system). In the present investigation it was found that E_g values increase from 2.1 to about 2.27 eV as the rf power increases from 20 to 80 W and then decreases to 1.92 eV with further increase of power to 100 W while keeping the other process parameters constant. The bandgap of 2.27 eV is exhibited by a film deposited at 80 W of power. This film also shows high crystalline fraction and conductivity with lower activation energy. In a study by Wang *et al* [11], the values of E_g increase with the increase of nanoclusters of nc-Si:H in the a-Si:H matrix. Also Vasiliev *et al* [7] have used time-dependent local density approximation (TDLDA) to show the increases of E_g with the decrease of cluster size in the silicon nanostructures. In earlier studies in our laboratory, E_g values between 2.0 and 2.1 eV have been observed in a-Si:H films deposited in the second chamber of a cascaded glow discharge [22].

There exist ambiguities about the bandgap of nanocrystalline silicon films because the existing models show large variation in bandgap among themselves. Since, hydrogenated nanocrystalline silicon contains both amorphous and crystalline phases and their properties vary with the volume fraction of these phases. For the optical bandgap estimation, Tauc's [23] and Cody's [24] methods are generally employed. Tauc's gap shows higher values (as shown in figure 2(b)) of bandgap as compared to the value obtained by Cody (not shown here). But there is no clear physical principle to choose either model to estimate the optical bandgap. There is a publication by Wang *et al* [11] who have used the Tauc plot for obtaining the bandgap of nc-Si:H films having crystalline fraction variation from 24% to 75%. Rotaru *et al* [25] have observed a relation between optical bandgap and the content of amorphous silicon (in the range of 30–100%) in polycrystalline silicon using both Cody's and Tauc's models. It could be about the non-validity of Tauc's and Cody's models for the estimation of the optical bandgap for a high crystalline fraction containing silicon films. For simplicity, the E_{04} method where the absorption coefficient (α) of 10^4 is usually used shows a higher value of the optical bandgap. It is found that, by applying these models, there is variation in the values of the bandgap. However, the trend in bandgap variation with power of the deposited films remains the same. Investigation using the Penn bandgap [27] and Wemple and DiDomenico models [28] should be seen in the framework of the dielectric constant (ϵ) of these materials and how ϵ changes with the change in crystalline fraction in these films: subsequently its correlation with the bandgap would be interesting. Sharma [26] has calculated the size-dependent energy bandgap within the Penn model [27] of a nanocrystallite semiconductor. The bandgap of hydrogenated amorphous silicon is between 1.7 and 1.8 eV. But in the case of a mixed phase of crystalline (large grain size) and amorphous, i.e. microcrystalline phase, the bandgap should lie between amorphous and crystalline silicon. In the present investigation, however, the

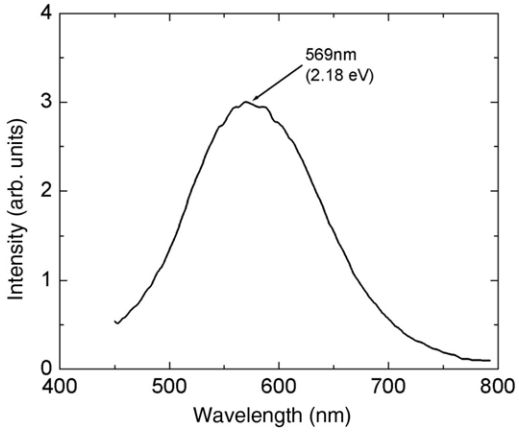

Figure 3. Typical photoluminescence spectra of an nc-Si:H film deposited using Ar dilution at a relative partial pressure of 0.25 Torr at 60 W power.

bandgap of the films is more than 1.9 eV. Bandgap broadening occurs in the materials if the quantum size effect prevails. Otherwise many other parameters must be looked at for the justification of bandgap broadening. A complete microscopic understanding of the bandgap depended on the fraction and size of nanocrystallites in the amorphous silicon matrix is still lacking. However, one of the well-accepted models for bandgap broadening for nanometric materials is quantum confinement [29].

The PL studies were carried out on nc-Si:H films deposited at 60 W rf power and Ar dilution at a relative partial pressure of 0.25 is shown in figure 3. The thickness of this film was ∼0.7 μm. The nc-Si:H film was exposed to ultraviolet excitation which contributed a very strong and broad emission peak at 569 nm (2.18 eV) with a bandwidth of 150 nm. The PL spectra confirm the high E_g estimated by Tauc's plot for our nc-Si:H silicon film. The PL peak value may not be confirmation of E_g. However, there is a research publication which showed that there is a relationship between the PL peak and bandgap [30]. This is in accordance with the previously reported theoretical studies where it has been mentioned that the quantum confinement effect broadened the E_g of nanocrystallites [7], increasing in oscillator strength giving rise to efficient and visible luminescence. However, the mechanism of the observed visible PL is not well understood. Some researchers attribute the PL to quantum size effects due to the silicon nanostructures [31–33], while others attribute it to hydrides/polysilanes [34, 35], siloxene [36, 37], oxygen-related defect centers [38–40] and amorphous silicon [41, 42]. There was no signature of oxygen in the film showing PL as confirmed from Fourier transform infrared spectroscopy measurements. We have estimated the particle size of a film showing a PL peak at 2.18 eV as 8.24 nm, using the relation [43] $D_L = h\pi/[2m_r(E_{PL} - E_g)]^{1/2}$, where D_L is the particle size, E_{PL} is the PL peak energy, $m_r[m_e m_h/m_e + m_h]$ is the reduced mass and E_g is the bulk silicon bandgap energy. The value of particle size is lower than the values observed in AFM images. This shows that there could be smaller grains embedded in large grains.

AFM images of nc-Si:H films deposited using 60, 80 and 100 W of applied power are shown in figure 4. Grain sizes of these images were estimated to be in the range 20–100 nm. The AFM micrograph deposited at 60 and 80 W powers as shown in figures 4(a) and (b) clearly reveals that there are small grains embedded in larger grains. It is also clear from these AFM images that, with the increase of applied rf power from 60 to 80 W, the density of grains increases and it looks like the smaller grains form into clusters, that is they agglomerate, as shown in figure 4(b). It is clearly visible in these AFM images that the smaller clusters of nc-Si:H grains are bound together and formed into larger grains and all these are embedded in the amorphous matrix. However, there is a decrease of nanocrystallites and an increase of amorphous phase in the films deposited at 100 W applied power as revealed from figure 4(c). This is also revealed from figure 2 where at 100 W power there is a decrease of E_g which may be correlated with low nanocrystallites observed in the AFM micrograph as shown in figure 4(c). Further, as revealed in figures 4(a)–(c) and 2, there is a correlation between size and density of nanocrystallites with the bandgap of nc-Si:H.

Figure 5 shows Raman spectra of nc-Si:H thin films deposited at various rf powers. Normally for amorphous silicon, the strongest line at 475 cm^{-1} originates from a displacement of the bridging silicon atom along a line bisecting two tetrahedral units, whereas for c-Si the very narrow line at 520 cm^{-1} originates from transverse optical (TO) phonons. The Raman spectra at 516 cm^{-1} has been assigned as a signature for nanosized c-Si or hexagonal c-Si [44]. In our investigation, Raman spectra at 514 cm^{-1} could be a signature of silicon nanostructures deposited at 60 and 80 W. However, films deposited at 100 W power show more amorphous in nature as there is an emergence of a broader Raman peak around 480 cm^{-1} and a narrowing of the peak around 514 cm^{-1}. High power (100 W) affects the formation of nanocrystallites in the growing film and turns the structure into a more amorphous one. We have also estimated the crystallite size (in diameter, D_R) of nanocrystalline silicon using the Raman peak, as $D_R = 2\pi\sqrt{B/\Delta\nu}$, where B is 2.24 cm^{-1} nm^2 and $\Delta\nu$ is the frequency shift in units of cm^{-1}, which was defined as the difference between the observed peak-frequency value and 522 cm^{-1} [45]. D_R values were found to be 3.69 nm and 3.26 nm for films deposited at 60 W and 80 W, respectively, since the AFM images indicate typically 30 nm particles inside 100–200 nm aggregates. The particle size estimated from Raman spectra also indicates that the 30 nm particles could be aggregates of smaller particles. However, particle size estimated from PL and laser Raman spectra are quite different. As an example, the values estimated from PL and laser Raman spectra were 8.24 nm and 3.69 nm, respectively, for the film grown at 60 W rf power and Ar dilution at a relative partial pressure of 0.25 Torr.

The effect of temperature on conductivity of nanocrystalline silicon films is shown in figure 6. These measurements were performed on coplanar structures. There is a wide variation of room temperature conductivity (σ_{RT}) which is in the range of 3×10^{-11} Ω^{-1} cm^{-1}–2×10^{-4} Ω^{-1} cm^{-1} with the variation of power from 60 W to 100 W. It is interesting to note that films deposited at 80 W power shows the highest σ_{RT} values among the set of films. This particular film shows σ_{RT} close

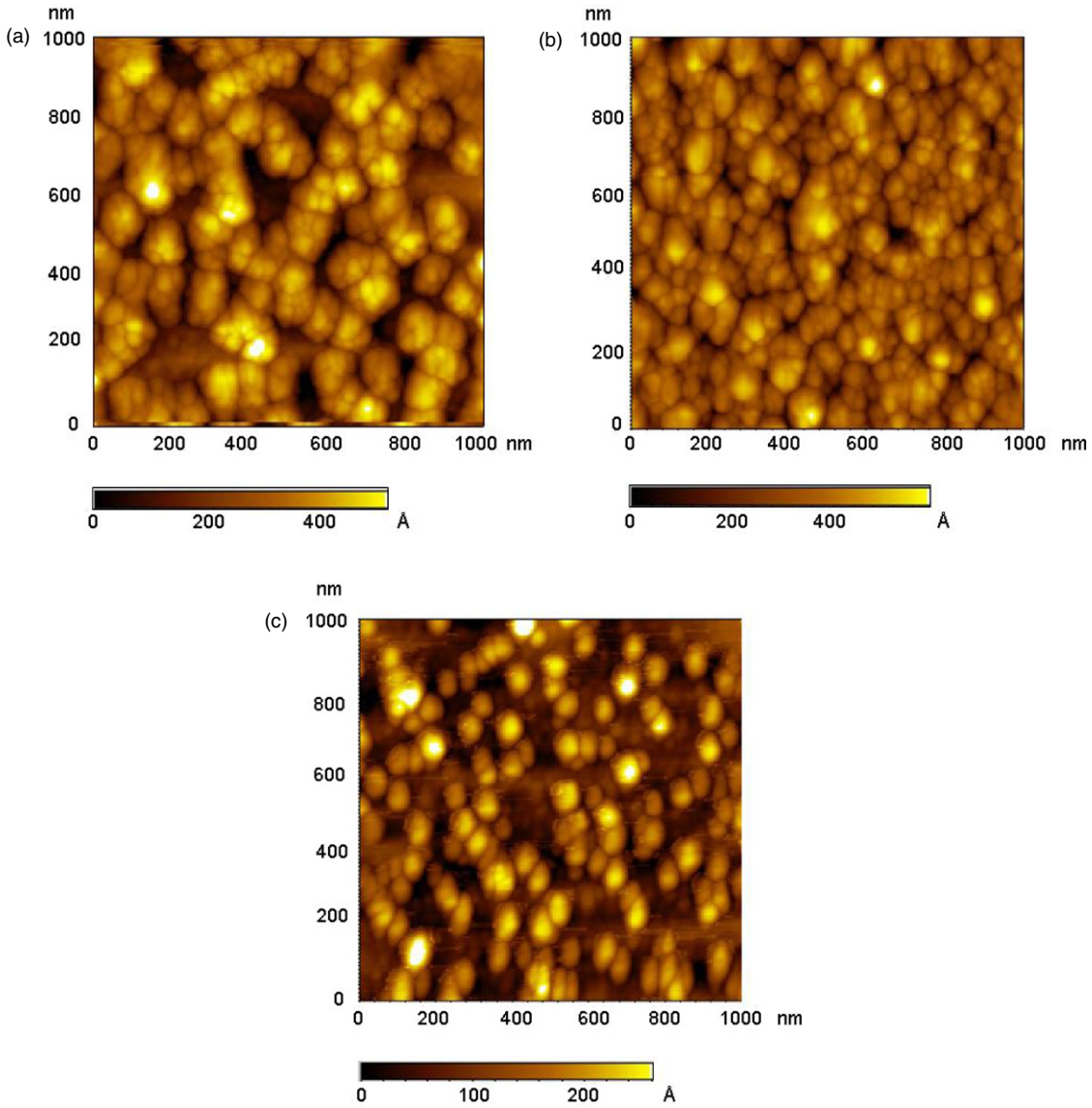

Figure 4. AFM micrograph of nc-Si:H films deposited at (a) 60 W, (b) 80 W and (c) 100 W power. (This figure is in colour only in the electronic version)

to 10^{-3} Ω^{-1} cm^{-1}, which is normally found for highly doped amorphous silicon films. It is confirmed from the morphological structure observed through AFM studies that the density of the nanocrystalline structure is greater in the film deposited at 80 W rf power. A similar result is also confirmed by laser Raman studies. The film deposited at 80 W power could be an optimum energy for the formation of maximum nanostructure which is responsible for the enhancement of conductivity. However, there is little change in dark to photoconductivity, i.e. photosensitivity observed at room temperature in the film deposited at 80 W. On the other hand photosensitivity was found up to 3–4 orders in the films deposited at 60 and 100 W power.

Films grown at 60 and 100 W power show multiple activation energies. However, films grown at 80 W power show two activation energies. The values of high activation energies (E_a) and pre-exponential factor (σ_0) were found to be 0.3 eV, 0.64 eV, 0.75 eV and 87 Ω^{-1} cm^{-1}, 12 Ω^{-1} cm^{-1}, 42 Ω^{-1} cm^{-1} for films deposited at 80 W, 60 W and 100 W power, respectively. The activation energy is presented for the higher temperature region. The increase of σ for 80 W deposited film is mainly due to the nanocrystalline nature of the film with small grains while other films deposited at 100 and 60 W are amorphous and partly crystallized with larger grains as revealed from Raman spectra.

The lower values of activation energy observed in films deposited at 80 W power may be due to the presence of a high density of nanostructure in the film and carrier transport occurred within these nanocrystallite grains connected with thin amorphous tissues which are embedded in the amorphous matrix. In other words the film consists of two types of structure, nanocrystalline and amorphous, and the smaller activation energies observed in these films could be due to the difference in bandgap of these two structures. They form heterojunction-like structures in the interface region, where the bandgap offset reduces the activation energy. Hu *et al* [46] have also observed an activation energy of 0.1–0.3 eV

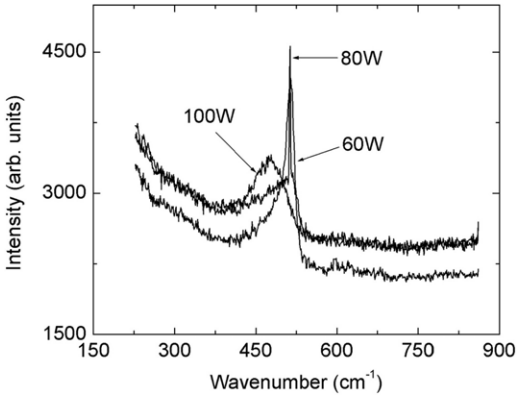

Figure 5. Laser Raman spectra of nc-Si:H films deposited at various powers.

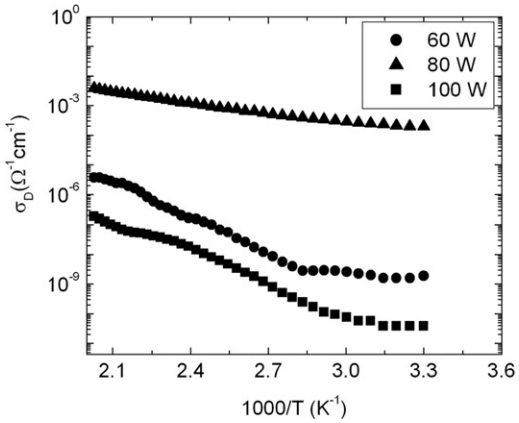

Figure 6. Conductivity as a function of temperature for nc-Si:H films deposited at various powers.

in their nc-Si:H films. The values of activation energies are lower than normally observed in a-Si:H films (0.8–0.9 eV). He *et al* [47] have suggested that the effective conductivity of nc-Si:H films is due to a two-phase random mixture of nc-Si:H films. One is the crystalline phase (many grains) and the other is the interface region (a-Si:H). We have seen in the present investigation that films deposited at 80 W show a high crystalline phase and thus higher conductivity. It has been shown that the conductivity of nc-Si:H films exponentially increases with increasing crystalline fraction and decreasing grain size [48]. A correlation between optical bandgap and activation energy of the nc-Si:H films can be seen, particularly for activation energies obtained for the higher temperature region in the present investigation. This could be due to the presence of nanocrystallites in the film which helps the broadening of the bandgap as well enhancement of the conductivity.

4. Conclusion

In conclusion, nc-Si:H films have been grown in the PECVD system using a gaseous mixture of SiH_4, H_2 and Ar in a high rf power regime, which is what one normally does not prefer to use for the growth of device quality a-Si:H films. These films were characterized for structural, optical and electrical properties as a function of applied rf power. E_g of these nc-Si:H films can be tailored by varying the rf power. It was observed that nanocrystallites in these films enhanced the optical bandgap and electrical conductivity. The values of E_g in these films were found to be in the range 1.9–2.3 eV. Temperature-dependent electrical conductivity has been measured and the activation energy was found to reduce to 0.3 eV in nc-Si:H films grown at an optimum power of 80 W. PL has been observed in these films in the visible region. PL emission in nc-Si:H is a highly desirable property for future advances in silicon-based electronic devices like blue LEDs and lasers. By proper optimization of the parameters one can obtain various color LEDs: red, green, yellow, maybe even white, as red, green, blue and white photoluminescence has already been observed from amorphous silicon quantum dots embedded in silicon nitride by controlling the dot size [49]. Optical bandgap and temperature-dependent electrical conductivity have been measured for these films. AFM images shows that these films contain nanocrystallites of 20–100 nm size in an amorphous matrix which is confirmed by the laser Raman peak at 514 cm^{-1} for these films. It is interesting to note that there are smaller nanocrystalline structures embedded in larger nanocrystalline grains as revealed from particle size estimation using PL (8.24 nm) and Raman (3.26 nm) spectra.

Acknowledgments

The authors would like to thank Dr Harish Chander for PL measurements from NPL, New Delhi and Professor S C Agarwal and his group from IIT Kanpur for providing laser Raman spectra and AFM images. We also acknowledge DST, Government of India for financial support to carry out this work.

References

[1] Veprek S and Marecek V 1968 *Solid State Electron.* **11** 683
[2] Xu G Y, Liu M, Wu X S, He Y L and Wang T M 1999 *J. Phys.: Condens. Matter* **11** 8495
[3] Binetti S, Acciarri M, Bollani M, Fumagalli L, Kanel H V and Pizzini S 2005 *Thin Solid Films* **487** 19
[4] Wu L, Huang X, Shi J, Dai M, Qiao F, Li W, Xu J and Chen K 2003 *Thin Solid Films* **425** 221
[5] Meier J, Fluckiger R, Keppner H and Shah A 1994 *Appl. Phys. Lett.* **65** 860
[6] Orpella A, Voz C, Puigodollers J, Dosev D, Fonrodona M, Soler D, Bertomeu J, Asensi J M, Andreu J and Alcubila R 2001 *Thin Solid Films* **395** 335
[7] Vasiliev I, Ogut S and Chelikowsky J R 2001 *Phys. Rev. Lett.* **86** 1813
[8] Street R A 1991 *Hydrogenated Amorphous Silicon* (Cambridge: Cambridge University Press)
[9] Kumar S, Gope J, Kumar A, Parashar A, Rauthan C M S and Dixit P N 2008 *J. Nanosci. Nanotechnol.* **8** 4211
[10] Dixit P N, Panwar O S, Satyanarayan B S and Bhattacharyya R 1995 *Sol. Energy Mater. Sol. Cells* **37** 143
[11] Wang Y H, Lin J and Huan C H A 2003 *Mater. Sci. Eng.* B **104** 80
[12] Klein S, Finger F, Carius R, Dylla T, Rech B, Grimm M, Houben L and Stutzmann M 2003 *Thin Solid Films* **430** 202

[13] Saleh R and Nickel N H 2003 *Thin Solid Films* **427** 266
[14] Shah A, Vallat-Sauvain E, Torres P, Meier J, Kroll U, Hof C, Droz C, Goerlitzer M, Wyrsch N and Vanecek M 2000 *Mater. Sci. Eng.* B **69/70** 219
[15] Kondo M, Fukawa M, Guv L and Matsuda A 2000 *J. Non-Cryst. Solids* **266–269** 84
[16] Roca i Cabarrocas P 2002 *Pure Appl. Chem.* **74** 359
[17] Roca i Cabarrocas P, Gay P and Hadjadj A 1996 *J. Vac. Sci. Technol.* A **14** 655
[18] Ghidini R, Groothuis C H J M, Sorokin M, Kroesen G M W and Stoffels W W 2004 *Plasma Sources Sci. Technol.* **13** 143
[19] Kortshagen U and Bhandarkar U 1999 *Phys. Rev.* E **60** 887
[20] Watanabe Y, Shiratani M and Koga K 2002 *Plasma Sources Sci. Technol.* A **11** 229
[21] Chaudhuri P, Meaudre R and Longeaud C 2004 *J. Non-Cryst. Solids* **338** 690
[22] Dixit P N, Bhattacharyya R, Panwar O S and Shah V V 1984 *Appl. Phys. Lett.* **44** 991
[23] Tauc J, Grigorovici R and Vancu A 1966 *Phys. Status Solidi* **15** 627
[24] Cody G D 1981 *Phys. Rev. Lett.* **47** 1480
[25] Rotaru C, Nastase S and Tomozeiu N 1999 *Phys. Status Solidi* a **171** 365
[26] Sharma A C 2006 *J. Appl. Phys.* **100** 084301
[27] Penn D R 1962 *Phys. Rev.* **128** 2093
[28] Wemple S H and DiDomenico M Jr 1971 *Phys. Rev.* B **3** 1338
[29] Sun C Q, Chen T P, Tay B K, Li S, Huang H, Zhang Y B, Pan L K, Lau S P and Sun X W 2001 *J. Phys. D: Appl. Phys.* **34** 3470
[30] Milovzorov D E, Ali A M, Inokuma T, Kurata Y, Suzuki T and Hasegawa S S 2001 *Thin Solid Films* **382** 47
[31] Canhan L T 1991 *Appl. Phys. Lett.* **57** 1046
[32] Wilson W L, Szayowski P F and Brus L E 1993 *Science* **1242** 262
[33] Dinh L N, Chase L L, Balooch M, Siekhans W J and Wooten F 1995 *Phys. Rev.* B **54** 5029
[34] Prokes S M, Glembocki O J, Bermudez V M, Kaplan R, Friedesdorf L E and Searson P C 1992 *Phys. Rev.* B **45** 13788
[35] Li K H, Tsai C, Sarathy J and Campbell J C 1993 *Appl. Phys. Lett.* **62** 3192
[36] Tse J S, Dahn J R and Buda F 1995 *J. Appl. Chem.* **99** 1896
[37] Brandt M S, Fuch H D, Stuzmann M, Weber J and Cardona M 1992 *Solid State Commun.* **81** 302
[38] Morisaki H, Hashimoto H, Ping E W, Nozawa H and Ono H 1933 *Appl. Phys. Lett.* **27** 2927
[39] Prokes S M and Carlos W E 1995 *J. Appl. Phys.* **78** 2671
[40] Prokes S M and Glemocki O J 1994 *Phys. Rev.* B **49** 2238
[41] Vasquez R P, Fathauer R W, George T, Ksendzow A and Lin T L 1992 *Appl. Phys. Lett.* **60** 1004
[42] George T, Anderson M, Pike W T, Lin T L, Fathauer R W, Jung K H and Wong D L 1992 *Appl. Phys. Lett.* **60** 2359
[43] Milovzorov D, Inokuma T, Kurata Y and Hasegawa S 1998 *Electrochem. Soc.* **145** 3615
[44] Anastassakis E and Liarokapis E 1987 *J. Appl. Phys.* **62** 3346
[45] Edelberg E, Bergh S, Naone R, Hall M and Aydil E S 1997 *J. Appl. Phys.* **81** 2410
[46] Hu G Y and Connell R F O 1995 *J. Appl. Phys.* **78** 3945
[47] He Y, Wei Y, Zheng G, Yu M and Liu M 1997 *J. Appl. Phys.* **82** 3408
[48] He Y, Yin C, Cheng G, Wang L and Liu X 1994 *J. Appl. Phys.* **72** 797
[49] Park N M, Kim T S and Park S J 2001 *Appl. Phys. Lett.* **78** 2575